Indices of abundance in the Gulf of Mexico reef fish complex: A comparative approach using spatial data from vessel monitoring systems

Nicholas D. Ducharme-Barth [a,*], Kyle W. Shertzer [b], Robert N.M. Ahrens [a]

[a] University of Florida, School of Forest Resources and Conservation, Program in Fisheries and Aquatic Sciences, 7922 NW 71st Street, Gainesville, FL 32653, USA.

[b] National Oceanic and Atmospheric Administration, Southeast Fisheries Science Center, 101 Pivers Island Road, Beaufort, NC 28516, USA

Abstract

The Gulf of Mexico reef fish complex is socioeconomically important and is exploited by a vertical line fishery capable of high resolution spatial targeting. Indices of abundance derived from fishery dependent catch-per-unit-effort (CPUE) data are an important input to the assessment of these stocks. Traditionally, these indices have been derived from standardized logbook data, aggregated at a coarse spatial scale, and are limited to generating predictions for observed spatiotemporal strata. Understanding how CPUE is spatially distributed, however, can help identify range contractions and avoid hyperstability or hyperdepletion, both of which can mask the true population dynamics. Vessel monitoring systems (VMS) can provide complete, high-resolution distributions of CPUE used to create abundance indices. Here we compare two methods — spatial averaging of VMS-derived catch and effort data and the result of generalized linear models applied to logbook data for generating indices, to evaluate the use of VMS-derived abundance indices in assessments of reef fish stocks. This work suggests that in fisheries where targeting occurs at very fine spatial scales, abundance indices derived from high-resolution, spatiotemporally complete data may more accurately reflect the underlying dynamics of the stock.

Keywords: CPUE standardization; vessel monitoring systems; reef fish; abundance index; simulation; Gulf of Mexico

* Corresponding author.
E-mail addresses: n.ducharmebarth@ufl.edu (N.D. Ducharme-Barth), kyle.shertzer@noaa.gov (K.W. Shertzer), rahrens@ufl.edu (R.N.M. Ahrens)

1. Introduction

Abundance indices are an important input for stock assessments. Fisheries-dependent data, such as catch-per-unit-effort (CPUE), are a common source of information for estimating trends in abundance, as they typically represent a more spatiotemporally complete and cost effective sample than fisheries-independent data (Ward, 2005).

Despite the availability of fishery dependent data, they may not be reliable as catch rates may not adequately track abundance. Nominal CPUE are widely regarded as disproportionate to abundance (Beverton and Holt, 1957; Harley et al., 2001) due to hyperstability - abundance declining faster than CPUE, or hyperdepletion - CPUE declining faster than abundance (Hilborn, and Walters 1992). These sources of non-linearity between CPUE and abundance can be introduced through gear effects (saturation and handling time; Deriso and Parma, 1987)), changes in fishing power (Bishop et al., 2004; Ye and Dennis, 2009), and interference between vessels (Gillis and Peterman, 1998). In addition, discrepancies between the spatial distributions of species abundance and fishing effort can exacerbate the issue if fishers are not representatively sampling the underlying abundance distributions (Clark and Mangel, 1979; Paloheimo and Dickie, 1964; Rose and Kulka, 1999; Rose and Leggett, 1991; Swain and Sinclair, 1994).

Bias in the relationship between CPUE and inferred abundance due to spatial distributions are typically addressed using one of two approaches: standardization or spatial imputation. Catch rates can be standardized using generalized linear models (GLMs) (Maunder and Punt, 2004; Nelder and Wedderburn, 1972) to separate the abundance trend from other factors. If spatial nominal CPUE data are available, they can be used to infer abundance trends provided they are spatially and/or temporally imputed to account for unfished areas and changes in the distributions of fishing effort (Walters, 2003). Abundance indices generated from spatially imputed nominal CPUE data that randomly sample the entire underlying distribution have been shown to track abundance accurately (Yu et al., 2013). However, for both of these approaches, the level of data aggregation is important to consider. Bias in the inferred abundance can occur if the level of data aggregation is too coarse such that fishing effort is no longer randomly sampling abundance within spatiotemporal strata (Campbell, 2004; Carruthers et al., 2010). Spatially averaging data on a fine spatial scale is more likely to represent the underlying abundance distribution of non-transient species (Carruthers et al., 2011).

Vessel monitoring systems (VMS) have transformed the analysis of fisheries-dependent spatial information. The high-resolution vessel location data provided by VMS have given fisheries scientists and managers a better understanding of the spatial distribution of effort (Lee et al., 2010; Mills et al., 2007), fisher behavior (Davie and Lordan, 2011; Vermard et al., 2010), and the abundance distributions of targeted stocks (Bertrand et al., 2008; Vinther and Eero, 2013). Linking self-reported logbook catch records to VMS data has allowed for the creation of species-specific distributions of CPUE in European trawl fisheries for groundfish (Gerritsen and Lordan, 2011; Witt and Godley, 2007) and the vertical line fishery targeting reef fish in the Gulf of Mexico (Ducharme-Barth and Ahrens, 2017).

The vertical line fishery in the Gulf of Mexico is a valuable commercial fishery (NMFS 2015, 2016) that targets a diverse complex comprised primarily of snappers, e.g. *Lutjanus spp*, and groupers, e.g. *Epinephelus spp* (Scott-Denton et al., 2011). The four most commercially encountered species (red snapper *Lutjanus campechanus*, vermilion snapper *Rhomboplites aurorubens*, red grouper *Epinephelus morio*, and gag grouper *Mycteroperca microlepis*) can be characterized by an association with easily identifiable hard bottom structure (Grimes, 1978; Grimes and Huntsman, 1980; Lindberg et al., 2006; Moran, 1988) and high site fidelity

(Coleman et al., 2010, 2011). The vertical line gear (multiple baited lines dropped vertically from a stationary or slowly drifting vessel) fished in multiple short sets (~20 minutes) allows for high resolution spatial targeting of the hard bottom structure and the targeted fish stocks (Pollack et al., 2013; SAFMC, 2009; Scott-Denton et al,. 2011). This combination of targeting behavior and species characteristics predisposes the fishery to the risk of hyperstability, particularly in the absence of spatial information on where catches occur.

Given the unique set of coinciding circumstances between vertical line fisheries and reef fish behavior, it is worthwhile to evaluate if developing abundance indices from higher resolution catch and effort data from VMS gives a more accurate approximation of the underlying abundance trends. Ideally, one would be able to work with data at a spatial resolution where sampling is representative of the underlying abundance (Walters, 2003). However, the fishing behavior of the vertical line fleet makes it unlikely that data aggregated at all but the finest scales (e.g. reef or artificial structure) meet this criterion. The current practice for generating abundance indices in this fishery is through the standardization of commercial logbook catch records aggregated to a coarse statistical grid, at best a 1 degree spatial grid, using a two-step delta-GLM (Lo et al., 1992; Stefansson, 1996). A delta-GLM is the product of two GLMs: a logistic model that describes the presence-absence of positive catches and an additional model (with normally distributed error structure in this case) that describes the magnitude of log(CPUE) for catches greater than 0. This paper evaluates two methods of creating abundance indices as applied in a vertical line fishery for reef fish, and more generally in fisheries able to achieve a high level of spatial targeting of non-transient species.

We conducted analyses to compare abundance indices derived from the same input catch data using two methods: the delta-GLM standardization (status-quo) and spatial averaging of VMS derived CPUE distributions. The first analysis evaluated the agreement between indices generated from the two methods utilizing as input commercial logbook catch records from a suite of reef fish stocks that make up a large proportion of the catch by the vertical line fleet in the Gulf of Mexico. Agreement was assessed in two ways: (i) by calculating the correlation between the indices from the two methods, and (ii) by calculating the change in abundance inferred by each method. Instances of poor agreement between the two methods provided motivation for determining which method more accurately tracked abundance.

A simulation analysis was used to assess how well each method captured the true population abundance trend under different effort and abundance scenarios. Corresponding catch and VMS records were simulated and passed as input to the two methods to create abundance indices. The deviations of the indices from the true trend were calculated to determine which method was more accurate under the various scenarios. A principal component analysis (PCA) identified characteristics of scenarios where there were large disparities in the accuracy of the two methods. Previous simulation studies investigated the effects of spatial aggregation, changing distribution of effort, and imputing unfished spatiotemporal strata on indices for pelagic fisheries standardized with GLMs (Campbell, 2004, 2015; Carruthers et al., 2010, 2011; Lynch et al., 2012). Other have studies investigated how geostatistical averaging of VMS-informed catch rates compared to a fisheries-independent measure of abundance in a scallop fishery (Walter et al. 2014a, b). This work represents the first direct comparison of abundance indices derived from delta-GLM standardization and spatial averaging of VMS derived CPUE distributions.

2. Material and Methods

This study aimed to address the potential fine-scale spatial targeting problem in conventional CPUE standardization by evaluating the use of VMS data for estimating population trends.

Multiple analyses, conduct in R 3.3.2 (R Core Team, 2016), were used to compare the delta-GLM and VMS methods. An overview of the fishery and the species included in the study can be found in section 2.1 and a description of the two data sources informing each method can be found in section 2.2. The first step was to use the same fisheries data to estimate abundance indices using the two methods for every study species. Detail on how abundance indices were constructed for each method can be found in section 2.3. The next step was to assess the agreement in species abundance indices estimated using the two methods. This was done using a non-parametric approach described in section 2.4. Calculating the agreement between indices constructed using the same catch data, but with different methodologies allowed us to identify if there were noticeable differences between the abundance indices created.

A simulation study was used to evaluate which method was more accurate in estimating abundance under a suite of scenarios governing how effort and abundance were distributed spatially. The base simulation described in section 2.5.1 was designed to simulate fine scale targeting in a multi-species fishery on a 1/12th degree spatial grid. Section 2.5.2 describes how the base simulation was modified for each scenario. In each scenario, abundance indices for each species were calculated using the two methods along with the deviation from the true simulated population trend (described in section 2.5.3). This allowed us to identify how sensitive the accuracy of each method was with respect to changes in broad patterns of effort and abundance. A multivariate analysis (described in section 2.5.4.) was used to identify the effort and abundance characteristics of species-scenario combinations where the two methods predicted diverging abundance trends.

The base simulation made the simplifying assumption that sampling by the fishery did not affect abundance, as this feedback was not necessary in the direct comparison of the ability of the two methods to handle fine-scale spatial data. However, making this assumption ignored the potential effects of in-year sequential depletion occurring at scales smaller than the spatial grid used in the simulation. Hyperstability could occur in fisheries targeting small aggregations or reefs within a cell if vessels move from reef to reef fishing down each in turn. A modification to the base simulation (described in Section 2.5.5) was used to explore how sequential depletion at the cell level affected the estimated abundance indices' ability to capture the true abundance trend.

2.1. Study Frame

The study frame for this project was the vertical line reef fish fishery within the Gulf of Mexico EEZ (Fig. 1) during 2007– 2013. Vertical line fishing consists of dropping multiple baited hooks on a single line or multiple lines deployed vertically from a stationary or slowly drifting vessel. These lines are predominantly retrieved using mechanical means such as electric or hydraulic reels though they may also be retrieved by hand. Fishing occurs in distinct spatiotemporal sets defined as the period that hooks are being fished from a vessel at that location. Multiple drops of the gear can occur during each fishing set. A change in location or prolonged period with hooks out of the water represents a change to a new fishing set. Species were included in the analysis if they were within the top 25 of catch by weight over the study period (Table 1). Two pelagic species in the top 25 were excluded as they were likely targeted using non-vertical line gear.

2.2. Data

This study used two data sets: VMS-derived spatial CPUE and commercial logbook self-reported catch records (CLB). VMS use was required for all vessels holding a commercial Gulf of Mexico Reef Fish Permit starting in 2007,. Vessel positions are reported every 60 minutes at a resolution of ~0.1 meters. Reported positions were excluded from the analysis if they occurred outside of the study frame, were assumed not to represent fishing activity (<5 km from land), or corresponded to non-vertical line gear. The resulting data set contained 2,769,857 VMS entries spanning the study period (except for July and August 2010; these data were unavailable).

To determine whether the vessel positions corresponded to fishing activity, VMS points were classified as fishing or not fishing using a two-step random forest classification algorithm (Ducharme-Barth and Ahrens, 2017). A unit of effort in the fishery was defined to be a VMS point classified as fishing. Spatial distributions were generated at monthly intervals using the GPS information associated with each VMS entry. Effort points were aggregated on a $1/12^{th}$ degree spatial grid (roughly 10 km x 10 km). The species-specific catch in pounds for each trip in the CLB was uniformly distributed to all effort points associated with that trip. Spatial CPUE by species was defined in each grid cell as the total catch weight across all trips divided by the number of effort points across all trips.

A Monte Carlo simulation method was used to propagate classification uncertainty into the spatial distributions by generating 201 CPUE values for each grid cell. The method applied a two-step process that combined variability in the predicted state (fishing or not-fishing) for each VMS entry due to the random forest model and uncertainty in the predicted state accounting for the classification accuracy of the model. Thus, each of the 201 values represent an alternative fishing scenario that can be used to create an individual abundance index. The number of values, 201, generated for each cell was selected because variability across scenarios had stabilized when including more than 100 scenarios, and using greater numbers of scenarios became computationally challenging. Ducharme-Barth and Ahrens (2017) provide further detail of the VMS classification process and Monte Carlo simulation methods.

The second data source was the CLB records that corresponded to the VMS points. Within the study period, the CLB contained 31,643 unique vertical line fishing trips targeting reef fish. Trips were retained in the analysis if they indicated that a vertical line gear (hand line, hand gear, or hydraulic/electric reel) was used on that trip. A small percentage of retained trips (2%) indicated that multiple gears were used. Logbook variables considered for CPUE standardization included year, month, area fished, days away, number of crew, season, and region. Season was determined from month (1 – Jan, Feb, March; 2 – April, May, June; 3 – July, August, September; 4 – October, November, December). The region (Fig. 1) was assigned based on the reported area or statistical zone. Species CPUE by trip was defined as catch in pounds per hook-hours fished. Hook-hours fished is the product of number of lines fished, hooks fished per line, and total hours fished.

2.3. Abundance Indices

2.3.1. VMS

Annual abundance indices were created from VMS-derived spatial CPUE distributions for each of the 201 fishing scenarios using a combination of temporal imputation and spatial averaging (Walters, 2003). Within a fishing scenario, 82 monthly spatial CPUE distributions were computed to span the time series of seven years (minus two missing months). Cells were identified for temporal imputation if they were empty in a month but fished in another month. Empty cells were filled with the average value of that cell from the two previous months. If a cell was empty to begin the study period, but was fished in a later month, all months leading up to the first month fished were filled with the value of the first month fished. Following imputation, cell values were averaged within month to generate a monthly abundance index. For the two missing months of data (July and August 2010), CPUE was imputed as the average of the two adjoining months. The monthly abundance indices were summed within year to create the annual abundance indices. Repeating this process across fishing scenarios resulted in 201 annual abundance indices. This allowed for the calculation of uncertainty as the 95% inter-quantile range around the median for each year in the abundance index. The resulting indices were rescaled to Z scores e.g. mean of zero and standard deviation of one.

2.3.2. Delta-GLM (status-quo)

The most practical comparison would be between the VMS-derived abundance index and a corresponding commercial vertical line index used in the SouthEast Data, Assessment, and Review (SEDAR) process. The SEDAR process provides assessments for stocks in the southeast United States, including the Gulf of Mexico. Unfortunately, there was not a complete set of indices from the SEDAR process spanning the study period for all species. Additionally, variables used to standardize CPUE tended to vary slightly among different species (Bryan, 2013; Bryan and McCarthy, 2015; McCarthy, 2011; Saul, 2013; Smith et al., 2015; Smith and Goethel, 2015). For this study, species-specific indices derived from CLB data were created using a common framework that best approximated the various approaches used in the SEDAR process.

Abundance indices were created from CLB records corresponding to trips that likely encountered the target species. These trips were identified using a logistic regression model of multi-species presence-absence data taken from the CLB records (Stephens and MacCall, 2004). Then a delta-GLM (Lo et al., 1992; Stefansson, 1996) was used to standardize the log(CPUE) of the target species. Explanatory variables were selected for inclusion separately in each of the two delta-GLM sub-models according to Akaike information criterion (AIC), with the candidate variables being year, temporal strata (season or month), region, days away, and crew. All variables were categorical, and days away and crew number were binned (1,2,3,4,5,6,7,8,9,10+ and 1,2,3,4,5+ respectively). At minimum, the two sub-models had to contain a year effect, a temporal effect (season or month), and a region effect. Only one temporal effect could be considered in a sub-model at a time. All effects in the model were assumed to be fixed. Interactions between spatial and temporal strata were not considered as there were incomplete observations of strata combinations for some of the species considered. Imputing the catch rate of missing strata was not considered since this technique is not commonly used in the SEDAR process. To ensure that bias did not enter the delta-GLM parameter estimates due to the uneven distribution of observations across spatiotemporal strata in the models (Campbell, 2004), the observations were reweighted such that each spatiotemporal strata received equal weight in the models (Campbell, 2015).

The predictions for both sub-models across a table of all possible spatiotemporal strata (Walters, 2003) were multiplied together and back transformed from log space to give a single expected CPUE in each strata. For models where days away and crew were selected, the modal observation for that variable was used in all predictions across spatiotemporal strata (Campbell, 2015). Predictions within year were averaged across temporal strata (season or month) and a weighted average across regions was used to generate the annual abundance index (Campbell 2015). When averaging across regions, the assigned weights were proportional to the areas of the regions. The standard error for the annual abundance index was constructed from the uncertainties associated with the two sub-models according to the method described in Campbell (2015). Lastly, the indices were rescaled to Z scores.

2.4. Abundance index agreement

One of the purposes of this study was to assess the agreement between the indices generated from the two methods, VMS (***V***) and delta-GLM (***C***). We assess agreement using two methods: a standard metric of agreement, correlation, and a metric relevant to fishery managers that measures whether the two indices imply the same overall change in abundance.

Given the autocorrelation in time series data, a conventional calculation of correlation and significance would not be appropriate. To account for the auto-correlated nature of the data as well as the uncertainty in each index, we used a non-parametric modification of surrogate data testing to test if the temporal structure of the indices resulted in a meaningful correlation between the two methods. Surrogate data testing is a proof by contradiction technique used in time series analysis to detect non-linearity (Schreiber and Schmitz, 2000; Theiler et al., 1992). Surrogate data testing works by calculating a given metric for the original time series and comparing it to a distribution of metrics calculated from many surrogate data sets generated by some null model. If the metric from the original time series falls outside of the distribution of metrics from the surrogate data, then the original time series is different from the null model. In our case, because there is uncertainty around each time series, we compared two distributions to each other rather than a point estimate to a distribution. This modification is outlined in Fig. 2. For each pair of indices, ***V*** and ***C*** (Fig. 2 A), two new indices, ***v*** and ***c***, were created (Fig. 2 B):

$$(\mu \qquad) \tag{1}$$

$$(\mu \qquad) \tag{2}$$

where $\mu_{V,t}$ and $\mu_{C,t}$ correspond to the means of ***V*** and ***C*** at time *t*, and $\sigma_{V,t}$ and correspond to the standard errors of ***V*** and ***C*** at time *t*. The new indices, ***v*** and ***c***, account for the uncertainty associated with the abundance indices while maintaining the temporal structure of those indices. A Pearson's point-wise correlation can then be calculated between each pair of the indices ***v***, ***c***. Two surrogate indices, ***v'*** and ***c'***, can be formed by taking ***v*** and ***c*** and randomly rearranging their order (Fig. 2 C). A correlation is then calculated between each pair of the indices ***v'*** and ***c'***. Repeating the process of creating indices ***v***, ***c***, ***v'***, and ***c'*** (Fig. 2 B, C) 10,000 times resulted in a distribution of correlations where the temporal structure was preserved and a surrogate distribution of correlations where the temporal structure was rearranged (Fig. 2 D). The mode of the distribution where temporal structure was preserved gives the correlation between the two indices. Values closer to 1 show a positive correlation between indices and values closer to -1 show a negative correlation between indices.

The overlapping coefficient (OVL) is a commonly used metric for assessing the similarity between two distributions (Inman and Bradley, 1989; Rom and Hwang, 1996) and non-parametric estimates of OVL are robust to strong assumptions on the shape and variance of the distributions (Clemons and Bradley, 2000; Stine and Heyse, 2001). An OVL of 0 indicates the two distributions are completely dissimilar and an OVL of 1 indicates the two distributions are identical. The OVL, referred to as OVL_{Corr}, between the two distributions indicates the similarity of the correlations between the two indices accounting for the temporal autocorrelation and error associated with each index. In the current case, low OVL values indicate that the distributions of correlation with and without temporal structure are highly dissimilar and that the temporal structure resulted in a meaningful correlation. High OVL values indicate that a random temporal structure was just as likely to achieve the same level of correlation between indices.

We used the same 10,000 simulated indices, ***v*** and ***c***, to asses if both indices inferred the same change in stock abundance. Inferred change in stock abundance for each index was calculated as the difference between the mean of the first two years of the index and the mean of the last two years of the index. Each index was already scaled relative to its mean and standard deviation so this allowed for comparisons of the change in inferred stock abundance between indices. For each of the 10 000 indices the inferred change in stock abundance was calculated. This resulted in two distributions, one for the change in stock abundance inferred by the VMS method and the other for the change inferred by the delta-GLM method. The OVL, referred to as OVL_{Change}, between these two distributions was calculated. Low values of OVL indicated that the two distributions were dissimilar and that the two methods, VMS and delta-GLM, inferred different changes in stock abundance.

2.5. Simulation

2.5.1. Base simulation

To further evaluate the two methods, we designed a spatial simulation test to replicate the spatiotemporal dynamics of the underlying species abundance distributions and the vertical line fishery. A simulated fishing fleet was distributed across a multi-species fishery comprised of 15 species. Fishing and species abundance patterns were simulated at an annual scale for 7 years and across a 1/12th degree spatial grid.

The spatial distributions of abundance were simulated to be representative of reef fish species encountered in the Gulf of Mexico (Table 2). For each species, the base abundance distributions were smoothed versions of average annual distributions of spatial CPUE from the VMS data. Each base abundance distribution was rescaled to sum to 3×10^6 so that each species started the simulation with the same abundance. An annual abundance trend was applied to each species using a first order random walk:

(3)

where $a_{i,s,t}$ is the abundance of species *s* in cell *i* in year *t*, and ϵ is a normally distributed error term applied to each cell (ϵ is defined in more detail in Section 2.5.2.). Summing abundance across cells within years gave the true abundance trend for each species.

Fishing trips were simulated to be representative of the characteristics observed in the CLB and VMS datasets. The total number of trips, $TotalTrips_t$, in any given year *t* of the simulation was a random draw from the following distribution.

$$(\mu \quad 740) \tag{4}$$

Three variables defined each fishing trip f where : the number of VMS points or locations fished on a trip, ; the trip length in days, $DAYS_f$; and the number of crew, . The parameters used to define the distribution for these variables were estimated from the VMS and CLB data sets.

$$l(\mu \quad 06) \tag{5}$$

$$on(\lambda \quad 8) \tag{6}$$

$$ormal(\mu \quad 4) \tag{7}$$

In any trip, if 0 was drawn for any of these variables it was replaced with 1. Additionally, was rounded to the nearest integer value. The spatial distribution of effort was simulated by selecting an initial fishing location for each fishing trip, and then allowing additional movements to other cells for the remaining locations in VMS_f. The initial location or cell for a fishing trip was allocated in accordance with a simple gravity model such that near shore cells with high expected revenues had the greatest chance of being selected.:

$$\sum p \tag{8}$$

$$(d \qquad) \tag{9}$$

where was the initial cell for fishing trip *f* in year *t*, was the relative distance from shore in cell *i*, was the relative expected revenue in cell *i* in year *t*, and was the value of species *s* in year *t*. The annual value of species was taken as the average annual price per pound reported in the NOAA Annual Commercial Landing Statistics (NOAA, 2017). Movement to adjacent cells within a fishing trip was simulated according to a Queen's Case random walk with a 60% chance of staying in the same cell at each move. Out of bound cells were either on land or had a depth beyond 600m as either of these represent unlikely fishing locations for vertical line gear.

Each simulated fishing trip recorded the grid cells fished, the region corresponding to the initial fishing location, and the total catch of each species. The catch at each location, , was a function of abundance, , and vessel catchability, $Q_{f,i}$. The vessel catchability was defined by and a spatiotemporally correlated normally distributed random error, $\phi_{i,t}$.

$$\tag{10}$$

$$l(\mu \qquad 54) \qquad (0.8) \tag{11}$$

The parameters used to define and were selected so that the simulation produced realistic catch rates, representative of what the CLB data showed, given the scale of abundance. Additionally, we assumed that vessels with greater numbers of crew would be able to achieve higher catch rates because of reduced handling times. The species-specific catch was zero-inflated to account for occasions where no catches were made at that cell despite fishing effort. The error term $\phi_{i,t}$ was constructed as a first order random walk of Gaussian random fields (GRF) using the RandomFields package in R (Schlather et al., 2015):

$$GRF(\mu = 0, \sigma = 0.025, scale = 5) \tag{12}$$

2.5.2. Scenarios

The simulation applied a full factorial design considering three factors, each with two levels, resulting in eight scenarios (Table 3). To quantify variability, each scenario was simulated 100 times. The factors considered were species abundance pattern, how effort was distributed, and changes in spatial targeting. For the first factor, species included in the simulated fishery could have one of two abundance patterns, global or local. In the global case, the ϵ in Eq. (3) was the same for each cell. In the local case, ϵ was different for each cell and defined as a first order random walk of GRFs in the same way as $\phi_{i,t}$ but with $\sigma = 0.25$. This approach simulated a scenario where there were localized patterns in abundance due to regional patterns in oceanographic conditions. For the second factor of the simulation, effort was distributed in one of two ways. In the first case, there were no restrictions on the initial fishing location ($l_{f,t}$). The second case allocated $l_{f,t}$ to the four main spatial regions in proportion to the observed regional effort distribution from the fishery. This represented a scenario where vessels were unwilling to travel very far from their home port. The third factor controlled changes in spatial targeting by manipulating $r_{i,t}$ in the gravity model. The first case did not force a change in spatial targeting, and the values of $r_{i,t}$ were held constant across years. The second case forced a spatial targeting change midway through the simulation, by manipulating revenues ($p_{s,t}$) for two of the 15 species. The baseline values for species 7 and 9 were \$3.34/pound and \$2.65/pound, respectively. However, in this second case, in years 1-3 the value for species 9 was set to \$$10^7$/pound and in years 5-7 the value for species 7 was changed to \$$10^7$/pound. This had the effect of concentrating effort in the SEGOM region over the first three years of the simulation, opening the distribution of effort up in the fourth year, and then driving effort to the WGOM region in the final three years of the simulation. This case demonstrates an instance where the fishery dramatically changed its spatial targeting behavior due to changes in species desirability driven by regulatory or socioeconomic factors.

2.5.3. Abundance indices

Species-specific abundance indices were calculated for each simulation using the methods described in Section 2.3, albeit with slight changes accounting for simplifying assumptions made in the simulation. In the VMS method, spatial distributions of species CPUE were constructed at an annual scale by uniformly allocating $C_{f,s}$ across all cells visited by a specific trip. Temporal imputation followed the method in Section 2.3.1, but at an annual time step instead of a monthly time step. Species abundance indices were created by taking the average of each imputed annual CPUE distribution.

The simulation testing approach provided an opportunity to test the effects of spatial strata size and the inclusion of spatial interactions in the status-quo standardization procedure. Four delta-GLM formulations were used in each simulation to estimate abundance indices: large strata and no interactions (delta-GLM I), large strata with interactions (delta-GLM II), small strata and no interactions (delta-GLM III), and small strata with interactions (delta-GLM IV). The large strata correspond to the four main regions in the Gulf of Mexico (Fig. 1), and the small strata to the 10 subdivided regions (Fig. 1). Formulations with interactions allowed for sub-models that include year and region interactions to be included in the selection of the best model. Each of these formulations modified the same base delta-GLM. The base delta-GLM standardized log(CPUE) as a function of year, region, days away, and crew. CPUE from a given trip was defined at the set level as $C_{f,s}/VMS_f$.

Species abundance indices were created following Section 2.3.2. Trips from the simulated logbook that were likely to have targeted a given species were identified using the method of (Stephens and MacCall, 2004). CPUE from these trips were standardized using the delta-GLMs described in the previous paragraph. Inclusion of interaction terms in the construction of species abundance indices followed the suggestions made in Campbell (2015).

The ability of each method to capture the true trend was assessed in each simulation and for each species by calculating the root-mean-square deviation (RMSD) between the estimated abundance index and the true index. The RMSD between two indices is defined as:

$$\sqrt{\frac{\sum_{t=1}^{n}(es \qquad\qquad)}{\qquad}} \tag{13}$$

All indices, both true and estimated, were scaled relative to their means and standard deviations, making values of RMSD comparable across species and scenarios.

2.5.4. Multivariate analysis

We used a principal component analysis (PCA) to identify the characteristics of scenarios of particular concern where the two methods estimated diverging trends in abundance. PCA is a multivariate technique that clusters observations in ordination space (McGarigal et al., 2000), and gives meaning to where observations are positioned relative to each other based on the principal component axes and the included variables. Principal component axes are orthogonal compositions of the included variables, with each axis explaining some proportion of the total variability in the observations. When plotted, observations and variables with positive values for a given principal component indicate positive correlation with that axis, and conversely negative values for an axis indicate negative correlation. Nine variables (all scaled relative to their mean and standard deviation) characterizing the simulations (Table 4) were used in the PCA. The first two principal components, respectively explaining 37.91% and 15.39% of the total variability, were retained for this analysis.

2.5.5. Sequential depletion simulation

We made three modifications to scenario 6 (Table 3) of the base simulation to explore the potential effects of in-year sequential depletion on the method's ability to estimate the true abundance trend. We chose the effort and abundance patterns of scenario 6 as our baseline since it provided a realistic approximation of the fishery without drastic changes in spatial targeting. The three modifications were 1) within cell abundance ($a_{i,s,t}$) was distributed across reefs, 2) within cell effort was distributed across reefs, and 3) catches were subtracted from abundance at that reef within year. The number of fishable reefs in cell *i* was defined as a random draw from a Poisson distribution.

$$on(\lambda \quad 7) \tag{14}$$

If the value 0 was drawn for any cell, it was replaced with 1. In the base simulation, fished cells were visited approximately 4-5 times a year. We simulated the number of reefs per cell with λ = 7 to ensure the likelihood of sequential depletion occurring at the cell level. Cell abundance at the start of a year was randomly allocated across reefs associated with that cell. Effort characteristics and cells fished within each trip were simulated in the same way as in the base simulation. For each cell fished on a trip, a reef within that cell was then randomly selected using a multinomial distribution. The probability of selecting a particular reef within a cell was equal to the proportion of total cell abundance at that reef. Catch was then defined at the reef level according to equations 10 and 11, and then subtracted from the available abundance at that reef in that year. If the catch value generated by equation 11 was greater than the available abundance at that particular reef, the catch was set equal to the available abundance. Abundance indices were then calculated in the same way as described in Section 2.5.3 for the VMS and delta-GLM I methods. When calculating the RMSD, the true abundance was taken as the mean of the starting and ending abundances for each year.

3. Results

Using the same catch records, abundance indices (Fig. 3) were estimated for each species listed in Table 2 using both the VMS and delta-GLM methods. Those that showed the strongest degree of positive correlation and lowest OVL_{Corr} (Table 5) included two species that were subject to high levels of directed targeting across a wide expanse of available fishing grounds, red snapper and gag grouper, as well as two species that are caught in association with them, gray triggerfish and black grouper, respectively. In general, most species showed some level of positive correlation, with both approaches revealing similar trends, though values of OVL_{Corr} were notably large. The greater the combined uncertainty between the two approaches, the higher the OVL_{Corr} in the relationship even if the mean trajectories appeared to correlate visually, e.g., yellowtail snapper, hogfish, and mutton snapper. In these three cases, the delta-GLM I indices all showed greater uncertainty than the VMS. All three of these species have relatively restricted spatial distributions of catch in an area of the Gulf of Mexico (SEGOM) that is subject to lower levels of fishing effort relative to the other regions. A delta-GLM approach attempting to standardize abundance at the Gulf-wide scale, like that currently used, could estimate higher levels of uncertainty due to fewer observations in spatial strata outside of the geographic core of the species catch distributions.

Two species were of particular concern, red porgy and mangrove snapper, as the two methods appeared to estimate inverse trends. This was corroborated by looking at the overall change in stock abundance inferred by each method for these two species as the OVL_{Change} was zero for both. For both of these species the VMS method indicated an overall increase in stock abundance and the delta-GLM indicated an overall decrease. Additionally, there were 10 other species where the OVL_{Change} indicated meaningful differences ($OVL_{Change} < 0.05$) and/or inferred different patterns of stock abundance. Clearly, these conflicting results were driven by differences in how the data were standardized or how spatial information was handled. However, without knowing the true trend, it was impossible to determine which method provided more accurate estimation. This issue demonstrated the need for our simulation study.

The simulation generated 100 sets of catch and effort data across eight scenarios. Using each simulated data set, five abundance indices (VMS and delta-GLMs I-IV) were created for each species within each scenario. Of the 15 species included in the simulation, the results for five of them are shown as representative of the diversity of patterns exhibited across all species. Species 1-2 and 7-8 were characterized by broad spatial distributions, while species 9 had a very restricted spatial distribution. Additionally, species 7 and 9 were used in the target switching scenarios with effort switching on or off (respectively).

A clear pattern emerged in the simulated abundance indices (Fig. 4). The VMS indices (blue) were consistently able to track the true abundance (black) for each species, across scenarios. Of the three factors manipulated to create the scenarios, abundance pattern and spatial targeting shifts both negatively affected performance of the simulated delta-GLM I indices (red). As expected, changing the abundance pattern from global (scenarios 1-4) to local (scenarios 5-8) had a negative effect on the delta-GLM I performance, since that particular formulation was unable to account for asymmetrical changes in abundance at scales smaller than the considered strata. Introducing a shift in spatial targeting had a subtler effect on the delta-GLM I indices. These indices appeared to be biased high for species in time periods when they were directly or indirectly targeted with greater effort. This effect is most clearly shown in scenarios 3 and 4 across all species. Effort targeting increased in the first three years for species 9, in year 4 for species 1 and 2, and in the last 3 years for species 7 and 8. Manipulating the effort distribution by restricting it within certain regions did not appear to alter the ability of either method to distinguish the true trend.

Accounting for additional delta-GLM formulations offered improvement but did not change the overall pattern that VMS indices more closely approximated the true trend (Fig. 5). As expected, the formulations using the smaller spatial strata provided an improvement in the delta-GLM indices. Allowing for models with spatial-temporal interaction terms to be included in the model selection process had mixed results. In most cases, including interactions resulted in a best model that either improved or did not meaningfully change the fit, even if inclusion of interaction terms were unwarranted (global abundance scenarios). However, there were cases where the unwarranted inclusion of interaction terms resulted in a diminished ability to estimate the true trend. In scenarios (Fig. 4, scenarios 3-4 for species 9) where the species occupied a restricted spatial range, a spatial shift in targeting occurred, and small spatial strata were used in the delta-GLM; the AIC indicated a mis-specified model as the best performer, which resulted in poor estimation of the true trend.

In addition to evaluation of methods, the simulation study was also able to replicate the prediction of inverse trends first observed in the actual data (Fig. 4, Species 8). A multivariate visualization (Fig. 6) showed the particular abundance and effort characteristics associated with this observation. An abundance decline and range contraction occurred simultaneously with a shift in spatial targeting. This resulted in a case where simulated fishing effort became increasingly able to target "hot spots" of abundance even as the stock decreased in range and total abundance. The increased correlation between effort and abundance shown by the increasing trend in Lee's L supported this. This dynamic was likely what proved problematic in the delta-GLM approaches, as effort was sampling non-randomly within the spatial strata considered, and thus introducing upward-biased catches into the analysis.

Accounting for in-year sequential depletion did not appear to make a meaningful difference in the method's ability to estimate the true population trend. In-year decreases in abundance averaged -49.85 % (std. dev. = 5.94) across all 15 species and 100 sets of data. Comparing the RMSD of the two methods (VMS and delta-GLM I) from scenario 6 to those from the depletion scenario (Fig. 7) did not indicate deteriorations in either method, nor any change in their relative performances.

4. Discussion

This paper shows that in fisheries where non-transient species are easily targeted at fine spatial scales, spatial averaging of high resolution CPUE data provides a robust estimate of abundance trends. Even in simulated cases where there were pronounced shifts in both the spatial distributions of effort and abundance, the VMS indices could more closely track the true abundance pattern relative to the status-quo delta-GLM method. This may allow VMS indices to serve as a bridge across significant perturbing events that may alter the spatial targeting pattern of the fishery provided catchability has remained relatively constant during the transition. Additionally, the pairing of high-resolution spatial data with catch rate information can also lead to the creation of region-specific indices of abundance, which can be used as input in spatial stock assessments (Booth, 2000) and be an important layer (Babcock et al., 2005; St Martin and Hall-Arber, 2008) in the marine spatial planning process (Gilliland and Laffoley, 2008).

Inferences on species trends targeted in the vertical line fishery for reef fish in the Gulf of Mexico may be limited due to the unquantified impacts of changing management practices. The emergence of inverse trends in both the actual and simulated data indicates that a spatial shift may have occurred at either the species or fleet level and that the VMS index may more accurately reflect abundance. However, either method would be susceptible to bias if the implementation of an individual fishing quota system (IFQ) on the grouper-tilefish sector of the fishery in 2010 (GMFMC, 2008) resulted in a sudden shift in catchability due to quota consolidation among more efficient vessels (Yandle and Dewees, 2008) or increased rates of discarding so that landings data became uncorrelated with abundance (Turner, 1997). This issue could partially be addressed by crafting abundance indices from a reference fleet of vessels, with assumed constant efficiency, which fished before and after the implementation of the IFQ system. Improving knowledge of discarding behavior through mandatory reporting or increased observer coverage could also explain changes in catchability. In addition to the potential IFQ influences on catchability, the multi-species nature of the reef fish fishery in the Gulf of Mexico could also affect catchability as a result of substructure within the fleet. For example, there exist several sub-fleets within the fishery, including those targeting shallow-water grouper, red snapper, and deep-water species (Scott-Denton et al., 2011). Though all targeted species are susceptible to capture by vertical line gear, subtle differences in gear configuration among sub-fleets could result in differential species-specific catchabilities. If differences in catchabilities are large and sub-fleet distribution is non-random, spatial biases in catch rate could be introduced. A good understanding of vessel membership among sub-fleets would be critical to addressing this potential source of bias as abundance indices could be derived from the spatial CPUE distribution corresponding to each sub-fleet and then averaged together.

Though not explicitly accounted for, the VMS indices were robust to the simulated sources of variability in catchability in the form of trip-level uncertainty and regional trends. This is likely a function of how the nominal spatial CPUE distributions used for the creation of those indices were defined. In defining spatial CPUE across all trips at the grid cell level, individual trip or vessel effects were averaged out provided there were a large number of unique samples within that cell. A limited number of trips in a given cell could reintroduce a bias in catch rates due to trip or vessel effects. Imputing values for cells with limited numbers of trips using regression could diminish this source of bias in the spatial averaging process used to create the abundance indices.

Targeting species at spatial scales finer than what is modeled has the potential to introduce hyperstability due to sequential-depletion. The simulation used to explore the effects of sequential depletion was not exhaustive and it is possible that hyperstability occurred at the grid cell level, but was masked due to the variability in abundance across cells and/or across years. Future work is needed to further examine the issue of sequential depletion and how aggregation scale affects our ability to observe fine scale processes. The high-resolution nature of VMS data makes it uniquely positioned to address this issue as it allows for aggregation at the same spatial scale that targeting is occurring.

Abundance indices derived from using the delta-GLM method were shown to be just as effective provided that the model was correctly specified to match the scale and dynamics of the underlying population. Improperly specifying the delta-GLM through the inclusion of unwarranted interaction terms or the use of inappropriately sized spatial strata led to decreased predictive ability. Earlier studies showed that AIC may select an overly complex model as best from a pool of candidate models (Carruthers et al., 2010; Kadane and Lazar, 2004). This result arose in the simulation in some cases as interaction models were incorrectly selected when there was in fact only a global trend in abundance. In a worst case scenario, specifying a model with inappropriately large strata resulted in an inverse trend being predicted by the delta-GLM. Further simulation of that scenario with smaller strata did improve the mean RMSD, though it still did not achieve the accuracy of the VMS-derived approach.

In scenarios where the two methods appeared to be equally effective in tracking the true abundance trend, determined by their overlapping RMSD distributions, there still existed visual differences in predicted trend. Particularly in scenarios where a spatial shift in targeting occurred, slight anomalies were introduced in species trends using the delta-GLM method. This difference between the two approaches could be meaningful in a stock assessment, particularly if it causes the abundance trend to conflict with other data sources. Issues with conflicting data are generally dealt with by either dropping the offending data source or reweighting it in the model (Maunder and Piner, 2017). Given the importance placed on maintaining a fit to the abundance trend during the data weighting process (Francis 2011, 2017), changing the data weighting to better fit the anomalous time series could have a large impact on the assessment output (Maunder et al., 2017; Punt, 2017).

One of the advantages of the VMS approach is comparative simplicity. The only major decision required is specifying the imputation rule for filling in unfished areas. Though not an overly complicated model structure, a delta-GLM requires a relatively large amount of expert knowledge of the fishery to correctly specify the sub-models. Some of the decisions required include choice of variables used for standardizing CPUE, the number and size of spatial strata, whether to include interaction terms, imputation method for unfished strata combinations, model selection criteria, model error structure, and model effects structure. Additionally, a precursor to the application of a delta-GLM model is to identify trips targeting the focal species using a method such as that of Stephens and MacCall (2004). Currently, there is no general guidance regarding how changing the selected trips affects the estimated abundance index or associated uncertainty. Averaging across a spatial catch rate distribution comprising all available catch records avoids this potential added source of uncertainty.

An extension of the delta-GLM, the spatiotemporal delta-generalized linear mixed model (delta-GLMM) is growing in popularity, though it is limited to regions where commercial logbooks include high resolution spatial data at the individual fishing set or tow level (Thorson and Barnett, 2017; Thorson et al., 2015). These models have shown the ability to accurately track abundance trends in multi-species fisheries where vessel targeting behaviors occur at multiple spatial scales (Thorson et al., 2016), provided the estimation model is correctly specified. Until the data requirements for this approach are met through observer coverage or electronic logbooks, creating indices from VMS-derived spatial CPUE data appears to be a suitable stepping stone from more commonly used delta-GLM approaches. Alternatively, the VMS-derived spatial CPUE could be used as input for the spatiotemporal delta-GLMM models.

This analysis demonstrates the utility of using high resolution CPUE distributions derived from VMS data to generate indices of abundance. The VMS method is comparatively simpler than delta-GLMs, and robust to changes in species and effort distributions. This approach shows much potential to incorporate high resolution spatial information about the fishery, and ultimately to improve stock assessments of non-transient species such as reef fishes in the Gulf of Mexico.

5. Acknowledgements

This research was funded through the NOAA Fisheries - Sea Grant Population and Ecosystem Dynamics Fellowship (grant # NA15OAR4170182) awarded to N.D.D. and through the NOAA Fisheries – RTR program (grant # NA11NMF4550121). The authors thank A. Punt, T. Carruthers as well as an anonymous reviewer for their thoughtful commentary which improved the quality of this manuscript. The authors declare no conflict of interest in this research.

Figure Captions

Figure 1: The Gulf of Mexico EEZ with the spatial regions considered in the analysis. The colored areas denote the four main regions: western Gulf (WGOM), northern Gulf (NGOM), northeastern Gulf (NEGOM), and southeastern Gulf (SEGOM). The lines indicate the 10 subdivided regions for the smaller spatial strata considered.

Figure 2: Diagram explaining how to calculate the correlation between two indices (A). The uncertainty of the initial indices is shown by the shaded regions. For each index, a new index is created by resampling from the uncertainty of the initial index (B). A correlation is calculated between the two new indices and is shown in green. For each new index in B, an additional index is formed by rearranging the order (C). A correlation is calculated between the two rearranged indices and is shown in orange. The process shown in panels B and C is repeated 10 000 times resulting in the two distributions of correlations (D). The time series correlation of the two initial indices is given by the mode of the distribution of correlations with order preserved (green). The overlapping coefficient (OVL_{Corr}) is given by the overlap of the two distributions.

Figure 3: Indices of abundance with associated uncertainty constructed using the two methods. The blue corresponds to the VMS index with the median estimate and the 95% inter-quantile range shown. Red corresponds to the delta-GLM index with the mean and the 95% confidence intervals shown.

Figure 4: Simulated abundance indices for five selected species, where each line represents a different prediction. The black line is the true abundance. Blue corresponds to the VMS-derived index and red corresponds to the estimate from a delta-GLM I index. The scenario number is denoted in the top right corner of each panel.

Figure 5: Violin plots showing the RMSD between predicted and true abundance for five selected species. The black line inside each violin signifies the 95% inter-quantile range, the black bar the 50% inter-quantile range, and the white dot the median RMSD. Moving from left to right within each panel the violins correspond to each method: VMS, delta-GLM I, delta-GLM II, delta-GLM III, and delta-GLM IV. The scenario number is denoted in the top right corner of each panel.

Figure 6: Principal components biplot for six of the nine variables used in the analysis. The lines represent the different variables, and the colored dots represent each species-method-scenario combination. For the three trend variables, blue is decreasing, red is increasing, and yellow is stationary. For the abundance pattern blue signifies global trends and red signifies local trends. For the targeting pattern blue indicates no switch in spatial targeting and red indicates a switch in spatial targeting. For the remaining variable, blue shows a low RMSD and red shows a high RMSD. The large colored dots highlight scenarios 7 and 8 for species 8.

Figure 7: Violin plots showing the RMSD from Scenario 6 for two methods: VMS (blue) and delta-GLM I (red). The pair on the left are without simulated sequential depletion, and the pair on the right (shaded region) are with simulated sequential depletion.

References

Babcock, E.A., Pikitch, E.K., McAllister, M.K., Apostolaki, P., Santora, C., 2005. A perspective on the use of spatialized indicators for ecosystem-based fishery management through spatial zoning. ICES J. Mar. Sci. 62 (3), 469-476.

Bertrand, S., Diaz, E., Lengaigne, M., 2008. Patterns in the spatial distribution of Peruvian anchovy (Engraulis ringens) revealed by spatially explicit fishing data. Prog. Oceanogr. 79 (2-4), 379-389.

Beverton, R.J.H., Holt, S.J., 1957. On the dynamics of exploited fish populations. Fish Fish. Ser. 11, 1-537.

Bishop, J., Venables, W.N., Wang, Y.G., 2004. Analysing commercial catch and effort data from a penaeid trawl fishery - A comparison of linear models, mixed models, and generalised estimating equations approaches. Fish. Res. 70 (2-3), 179-193.

Booth, A.J., 2000. Incorporating the spatial component of fisheries data into stock assessment models. ICES J. Mar. Sci. 57 (4), 858-865.

Bryan, M., 2013. Standardized catch rates for gag grouper from the United States Gulf of Mexico commercial handline fishery during 1990-2009. SEDAR33-AW15. SEDAR. (Available from: http://sedarweb.org/sedar-33-assessment-workshop).

Bryan, M., McCarthy, K., 2015. Standardized catch rates for red grouper from the United States Gulf of Mexico vertical line and longline fisheries. SEDAR42-AW-02. SEDAR. (Available from: http://sedarweb.org/sedar-42-assessment-workshop).

Campbell, R.A., 2004. CPUE standardisation and the construction of indices of stock abundance in a spatially varying fishery using general linear models. Fish. Res. 70 (2-3), 209-227.

Campbell, R.A., 2015. Constructing stock abundance indices from catch and effort data: Some nuts and bolts. Fish. Res. 161, 109-130.

Carruthers, T.R., Ahrens, R.N.M., McAllister, M.K., Walters, C.J., 2011. Integrating imputation and standardization of catch rate data in the calculation of relative abundance indices. Fish. Res. 109 (1), 157-167.

Carruthers, T.R., McAllister, M.K., Ahrens, R.N.M., 2010. Simulating spatial dynamics to evaluate methods of deriving abundance indices for tropical tunas. Can. J. Fish. Aquat. Sci. 67 (9), 1409-1427.

Clark, C.W., Mangel, M., 1979. Aggregation and fishery dynamics - theoretical study of schooling and the purse seine tuna fisheries. Fish. Bull. 77 (2):, 317-337.

Clemons, T.E., Bradley, E.L., 2000. A nonparametric measure of the overlapping coefficient. Comput. Stat. Data. Anal. 34 (1), 51-61.

Coleman, F.C., Koenig, C.C., Scanlon, K.M., Heppell, S., Heppell, S., Miller, M.W., 2010. Benthic habitat modification through excavation by red grouper, Epinephelus morio, in the northeastern Gulf of Mexico. Open Fish Sci. J. 3, 1-15.

Coleman, F.C., Scanlon, K.M., Koenig, C.C., 2011. Groupers on the Edge: Shelf Edge Spawning Habitat in and Around Marine Reserves of the Northeastern Gulf of Mexico. Prof. Geogr. 63 (4), 456-474.

Davie, S., Lordan, C., 2011. Examining changes in Irish fishing practices in response to the cod long-term plan. ICES J. Mar. Sci. 68 (8), 1638-1646.

Deriso, R.B., Parma, A.M., 1987. On the odds of catching fish with angling gear. Trans. Am. Fish. Soc. 116 (2), 244-256.

Ducharme-Barth, N.D., Ahrens, R.N.M., 2017. Classification and analysis of VMS data in vertical line fisheries: Incorporating uncertainty into spatial distributions. Can. J. Fish. Aquat. Sci. 74 (11), 1749-1764, https://doi.org/10.1139/cjfas-2016-0181.
Francis, R., 2011. Data weighting in statistical fisheries stock assessment models. Can. J. Fish. Aquat. Sci. 68 (6), 1124-1138.
Francis, R.I.C.C., 2017. Revisiting data weighting in fisheries stock assessment models. Fish. Res. 192, 5-15.
Gerritsen, H., Lordan, C., 2011. Integrating vessel monitoring systems (VMS) data with daily catch data from logbooks to explore the spatial distribution of catch and effort at high resolution. ICES J. Mar. Sci. 68 (1), 245-252.
Gilliland, P.M., Laffoley, D., 2008. Key elements and steps in the process of developing ecosystem-based marine spatial planning. Mar. Policy 32 (5), 787-796.
Gillis, D.M., Peterman, R.M., 1998. Implications of interference among fishing vessels and the ideal free distribution to the interpretation of CPUE. Can. J. Fish. Aquat. Sci. 55 (1), 37-46.
GMFMC, 2008. Amendment 29 to the Reef Fish Fishery Management Plan: Effort Management in the Commercial Grouper and Tilefish Fisheries. GMFMC, Tampa, FL. (Available from: http://gulfcouncil.org/fishery-management/implemented-plans/reef-fish/)
Grimes, C.B., 1978. Age, Growth, and Length-Weight Relationship of Vermilion Snapper, Rhomboplites-aurorubens from North-Carolina and South-Carolina Waters. Trans. Am. Fish. Soc. 107 (3), 454-456.
Grimes, C.B., Huntsman, G.R., 1980. Reproductive-Biology of the Vermilion Snapper, Rhoboplites-aurorubens, from North-Carolina and South-Carolina. Fish. Bull. 78 (1), 137-146.
Harley, S.J., Myers, R.A., Dunn, A., 2001. Is catch-per-unit-effort proportional to abundance? Can. J. Fish. Aquat. Sci. 58 (9), 1760-1772.
Hilborn, R., Walters, C.J., 1992. Quantitative fisheries stock assessment choice dynamics and uncertainty. Chapman and Hall, New York.
Inman, H.F., Bradley, E.L., 1989. The overlapping coefficient as a measure of agreement between probability distributions and point estimation of the overlap of two normal densities. Commun. Stat. Theory Methods 18 (10), 24.
Kadane, J.B., Lazar, N.A., 2004. Methods and criteria for model selection. J. Am. Stat. Assoc. 99 (465), 279-290.
Lee, J., South, A.B., Jennings, S., 2010. Developing reliable, repeatable, and accessible methods to provide high-resolution estimates of fishing-effort distributions from vessel monitoring system (VMS) data. ICES J. Mar. Sci. 67 (6), 1260-1271.
Lindberg, W.J., Frazer, T.K., Portier, K.M., Vose, F., Loftin, J., Murie, D.J., Mason, D.M., Nagy, B., Hart, M.K., 2006. Density-dependent habitat selection and performance by a large mobile reef fish. Ecol. Appl. 16 (2), 731-746.
Lo, N.C.H., Jacobson, L.D., Squire, J.L., 1992. Indexes of relative abundance from fish spotter data based on delta-lognormal models. Can. J. Fish. Aquat. Sci. 49 (12), 2515-2526.
Lynch, P.D., Shertzer, K.W., Latour, R.J. 2012. Performance of methods used to estimate indices of abundance for highly migratory species. Fish. Res. 125, 27-39.
Maunder, M.N., Crone, P.R., Punt, A.E., Valero, J.L., Semmens, B.X., 2017. Data conflict and weighting, likelihood functions and process error. Fish. Res. 192, 1-4.

Maunder, M.N., Piner, K.R., 2017. Dealing with data conflicts in statistical inference of population assessment models that integrate information from multiple diverse data sets. Fish. Res. 192, 16-27.

Maunder, M.N., Punt, A.E., 2004. Standardizing catch and effort data: a review of recent approaches. Fish. Res. 70 (2-3), 141-159.

McCarthy, K., 2011. Commercial Vertical Line Vessel Standardized Catch Rates of Yellowtail Snapper in southern Florida, 1993-2010. SEDAR27-DW11. SEDAR. (Available from: http://sedarweb.org/sedar-27-data-workshop).

McGarigal, K., Cushman, S., Stafford, S.G., 2000. Multivariate statistics for wildlife and ecology research. Springer, New York.

Mills, C.M., Townsend, S.E., Jennings, S., Eastwood, P.D., Houghton, C.A., 2007. Estimating high resolution trawl fishing effort from satellite-based vessel monitoring system data. ICES J. Mar. Sci. 64 (2), 248-255.

Moran, D., 1988. Species profiles: life histories and environmental requirements of coastal fishes and invertebrates (Gulf of Mexico)--red snapper. US FWS. (Available from: https://www.nwrc.usgs.gov/wdb/pub/species_profiles/82_11-083.pdf).

Nelder, J.A., Wedderburn, R.W., 1972. Generalized Linear Models. J. R. Stat. Soc. Ser. C. Gen. 135 (3), 370.

NMFS, 2015. Fisheries Economics of the United States, 2013. NOAA-Fisheries. (Available from: https://www.st.nmfs.noaa.gov/economics/publications/feus/FEUS-2013/fisheries_economics_2013).

NMFS, 2016. Commercial Landings by Gear. NOAA-Fisheries. (Available from: https://www.st.nmfs.noaa.gov/commercial-fisheries/commercial-landings/landings-by-gear/index).

NOAA, 2017. Commercial Fisheries Statistics: Annual Landings. NOAA-Fisheries. (Available from: http://www.st.nmfs.noaa.gov/commercial-fisheries/commercial-landings/annual-landings/index2017).

Paloheimo, J.E., Dickie, L.M., 1964. Abundance and fishing success. Rapp. P. V. Réun. CIEM 155, 12.

Pollack, A.G., Campbell, M.D., Driggers, W.B., 2013. Estimation of hook selectivity on red snapper (Lutjanus campechanus) during a fishery independent survey on natural reefs in the Gulf of Mexico. SEDAR31-AW12. SEDAR. (Available from: http://sedarweb.org/sedar-31-assessment-workshop).

Punt, A.E., 2017. Some insights into data weighting in integrated stock assessments. Fish. Res. 192, 52-65.

R Core Team, 2016. R: A Language and Environment for Statistical Computing. Vienna, Austria.

Rom, D.M., Hwang, E., 1996. Testing for individual and population equivalence based on the proportion of similar responses. Stat. Med. 15 (14), 1489-1505.

Rose, G.A., Kulka, D.W., 1999. Hyperaggregation of fish and fisheries: how catch-per-unit-effort increased as the northern cod (Gadus morhua) declined. Can. J. Fish. Aquat. Sci. 56, 118-127.

Rose, G.A., Leggett, W.C., 1991. Effects of biomass range interactions on catchability of migratory demersal fish by mobile fisheries - an example of atlantic cod (Gadus morhua). Can. J. Fish. Aquat. Sci. 48 (5), 843-848.

SAFMC, 2009. Fishery Ecosystem Plan of the South Atlantic Region Volume III: South Atlantic Human and Institutional Environment. South Atlantic Fishery Management Council. (Available from: http://safmc.net/ecosystem-library/volume-iii-human-and-institutional-environment/).

Saul, S., 2013. Commercial Indices of Abundance for Greater Amberjack in the Gulf of Mexico. SEDAR33-AW18. SEDAR. (Available from: http://sedarweb.org/sedar-33-assessment-workshop).

Schlather, M., Malinowski, A., Menck, P.J., Oesting, M., Strokorb, K., 2015. Analysis, Simulation and Prediction of Multivariate Random Fields with Package Random Fields. J. Stat. Softw. 63 (8), 1-25.

Schreiber, T., Schmitz, A., 2000. Surrogate time series. Phys. D 142 (3-4), 346-382.

Scott-Denton, E., Cryer, P.F., Gocke, J.P., Harrelson, M.R., Kinsella, D.L., Pulver, J.R., Smith, R.C., Williams, J.A., 2011. Descriptions of the U.S. Gulf of Mexico Reef Fish Bottom Longline and Vertical Line Fisheries Based on Observer Data. Mar. Fish. Rev. 73 (2), 1-26.

Smith, M.W., Goethel, D., Rios, A., Isley, J., 2015. Standardized Catch Rate Indices for Gulf of Mexico Gray Triggerfish (Balistes capriscus) Landed During 1993-2013 by the Commercial Handline Fishery. SEDAR43-WP-05. SEDAR. (Available from: http://sedarweb.org/sedar-43-dataassessment-workshop).

Smith, M.W., Goethel, D.R., 2015. Standardized Catch Rate Indices for Gulf of Mexico Vermilion Snapper (Rhomboplites aurorubens) Commercial Handline Fishery, 1993-2014. SEDAR45-WP-04. SEDAR. (Available from: http://sedarweb.org/sedar-45-dataassessment-workshop).

St Martin, K., Hall-Arber, M., 2008. The missing layer: Geo-technologies, communities, and implications for marine spatial planning. Mar. Policy 32 (5), 779-786.

Stefansson, G., 1996. Analysis of groundfish survey abundance data: Combining the GLM and delta approaches. ICES J. Mar. Sci. 53 (3), 577-588.

Stephens, A., MacCall, A., 2004. A multispecies approach to subsetting logbook data for purposes of estimating CPUE. Fish. Res. 70 (2-3), 299-310.

Stine, R.A., Heyse, J.F., 2001. Non-parametric estimates of overlap. Stat. Med. 20 (2), 215-236.

Swain, D.P., Sinclair, A.F., 1994. Fish distribution and catchability - what is the appropriate measure of distribution. Can. J. Fish. Aquat. Sci. 51 (5), 1046-1054.

Theiler, J., Eubank, S., Longtin, A., Galdrikian, B., Farmer, J.D., 1992. Testing for nonlinearity in time-series - the method of surrogate data. Phys. D 58 (1-4), 77-94.

Thorson, J.T., Barnett, L.A.K., 2017. Comparing estimates of abundance trends and distribution shifts using single- and multispecies models of fishes and biogenic habitat. ICES J. Mar. Sci. 74 (5), 1311-1321.

Thorson, J.T., Fonner, R., Haltuch, M.A., Ono, K., Winker, H., 2016. Accounting for spatiotemporal variation and fisher targeting when estimating abundance from multispecies fishery data. Can. J. Fish. Aquat. Sci. 74 (11), 1794-1807.

Thorson, J.T., Shelton, A.O., Ward, E.J., and Skaug, H.J., 2015. Geostatistical delta-generalized linear mixed models improve precision for estimated abundance indices for West Coast groundfishes. ICES J. Mar. Sci. 72 (5), 1297-1310.

Turner, M.A., 1997. Quota-induced discarding in heterogeneous fisheries. J. Environ. Econ. Manage. 33 (2), 186-195.

Vermard, Y., Rivot, E., Mahevas, S., Marchal, P., Gascuel, D., 2010. Identifying fishing trip behaviour and estimating fishing effort from VMS data using Bayesian Hidden Markov Models. Ecol. Modell. 221 (15), 1757-1769.

Vinther, M., Eero, M., 2013. Quantifying relative fishing impact on fish populations based on spatio-temporal overlap of fishing effort and stock density. ICES J. Mar. Sci. 70 (3), 618-627.

Walter, J.F., Hoenig, J.M., Christman, M.C., 2014a. Reducing Bias and Filling in Spatial Gaps in Fishery-Dependent Catch-per-Unit-Effort Data by Geostatistical Prediction, I. Methodology and Simulation. N. Am. J. Fish. Manag. 34 (6), 1095-1107.

Walter, J.F., Hoenig, J.M., Christman, M.C., 2014b. Reducing Bias and Filling in Spatial Gaps in Fishery-Dependent Catch-per-Unit-Effort Data by Geostatistical Prediction, II. Application to a Scallop Fishery. N. Am. J. Fish. Manag. 34 (6), 1108-1118.

Walters, C., 2003. Folly and fantasy in the analysis of spatial catch rate data. Can. J. Fish. Aquat. Sci. 60 (12), 1433-1436.

Ward, E.J., 2005. Differences between fishery-dependent and fishery-independent estimates of single-and mixed-species dolphin schools: implications for single-species stock assessments. Mar. Mamm. Sci. 21 (2), 189-203.

Witt, M.J., Godley, B.J., 2007. A Step Towards Seascape Scale Conservation: Using Vessel Monitoring Systems (VMS) to Map Fishing Activity. Plos One 2 (10).

Yandle, T., Dewees, C.M., 2008. Consolidation in an individual transferable quota regime: Lessons from New Zealand, 1986-1999. Environ. Manage. 41 (6), 915-928.

Ye, Y., Dennis, D., 2009. How reliable are the abundance indices derived from commercial catch-effort standardization? Can. J. Fish. Aquat. Sci. 66 (7), 1169-1178.

Yu, H., Jiao, Y., Carstensen, L.W., 2013. Performance comparison between spatial interpolation and GLM/GAM in estimating relative abundance indices through a simulation study. Fish. Res. 147, 186-195.

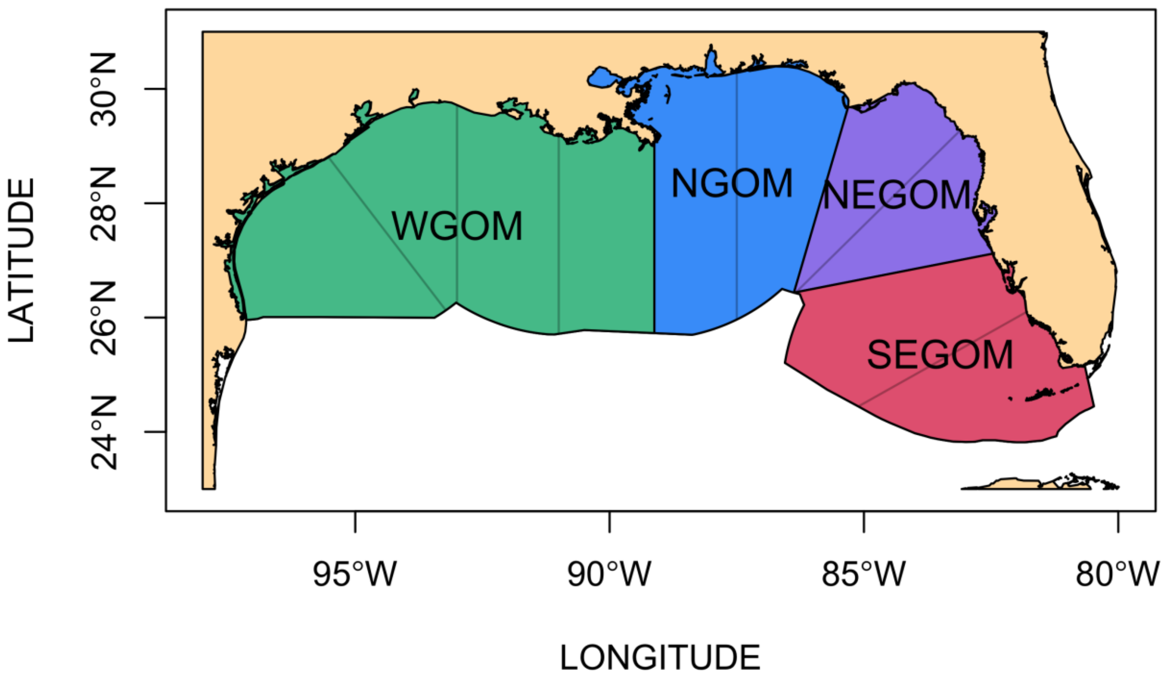
WGOM
NGOM
NEGOM
SEGOM
30°N
28°N
26°N
24°N
95°W
90°W
85°W
80°W
LATITUDE
LONGITUDE

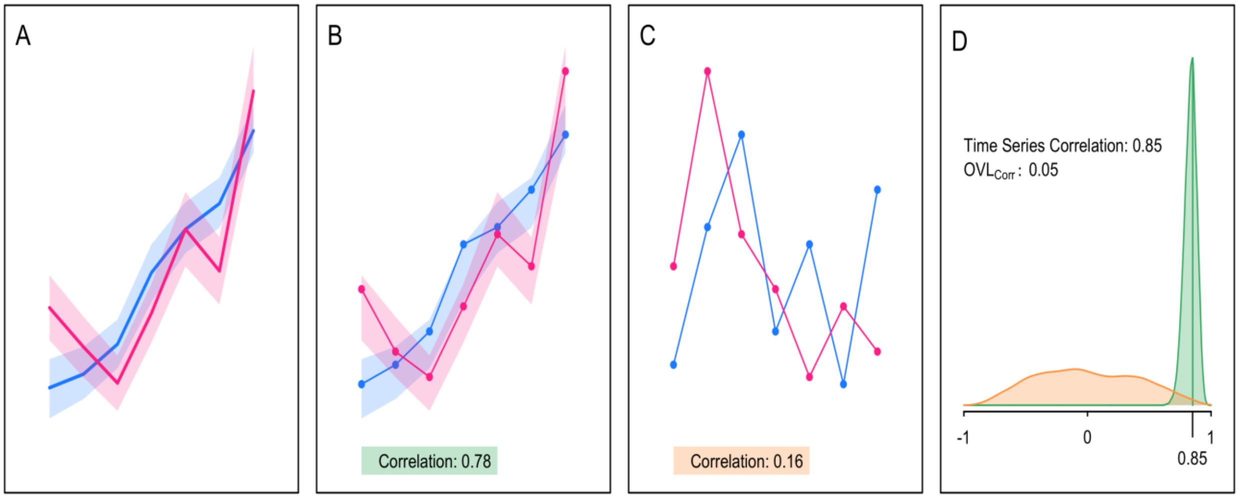
A
B
C
D
Correlation: 0.78
Correlation: 0.16
Time Series Correlation: 0.85
OVL$_{Corr}$: 0.05
-1
0
1
0.85

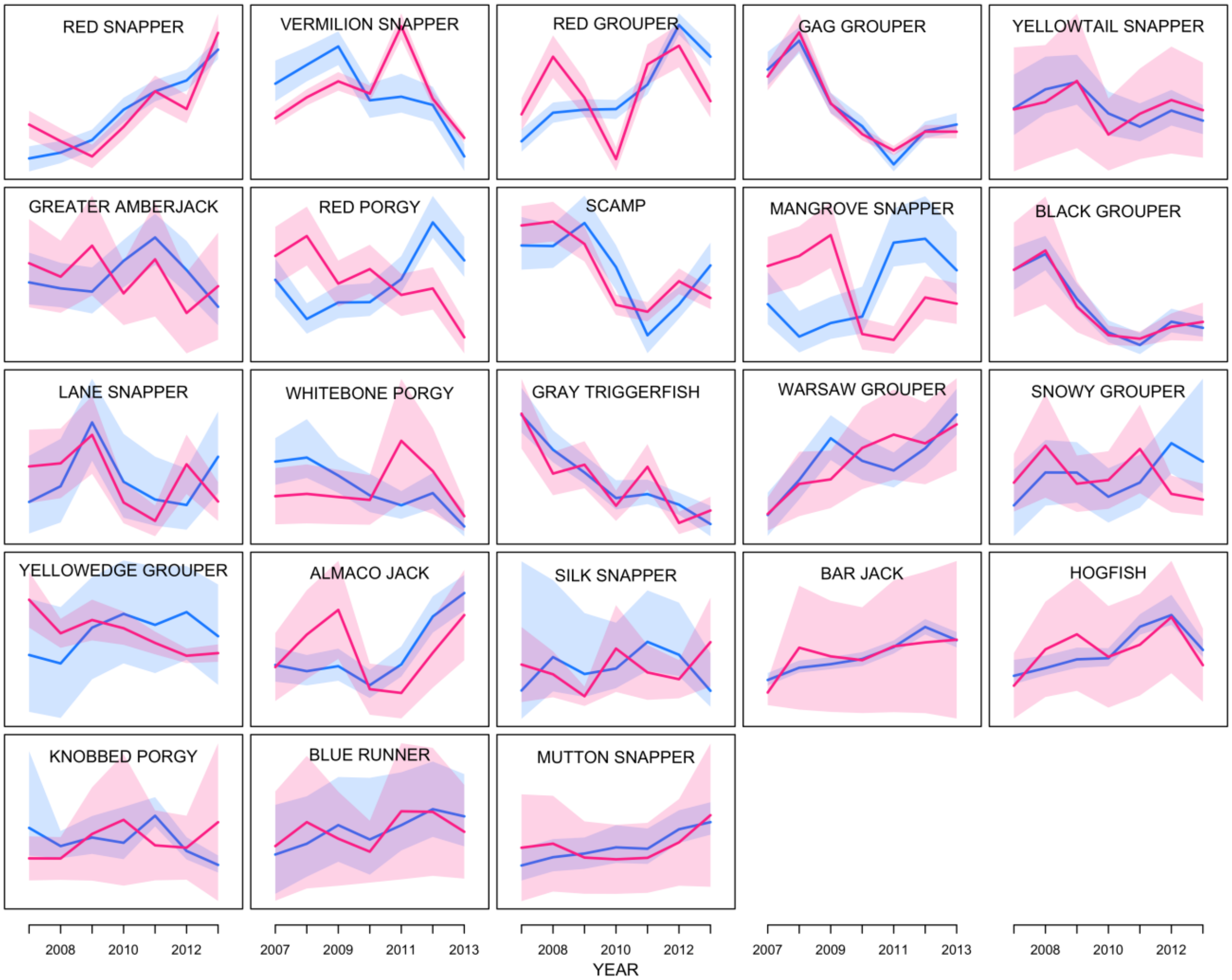
RED SNAPPER
VERMILION SNAPPER
RED GROUPER
GAG GROUPER
YELLOWTAIL SNAPPER
GREATER AMBERJACK
RED PORGY
SCAMP
MANGROVE SNAPPER
BLACK GROUPER
LANE SNAPPER
WHITEBONE PORGY
GRAY TRIGGERFISH
WARSAW GROUPER
SNOWY GROUPER
YELLOWEDGE GROUPER
ALMACO JACK
SILK SNAPPER
BAR JACK
HOGFISH
KNOBBED PORGY
BLUE RUNNER
MUTTON SNAPPER
2008 2010 2012
2007 2009 2011 2013
2008 2010 2012
2007 2009 2011 2013
2008 2010 2012
YEAR

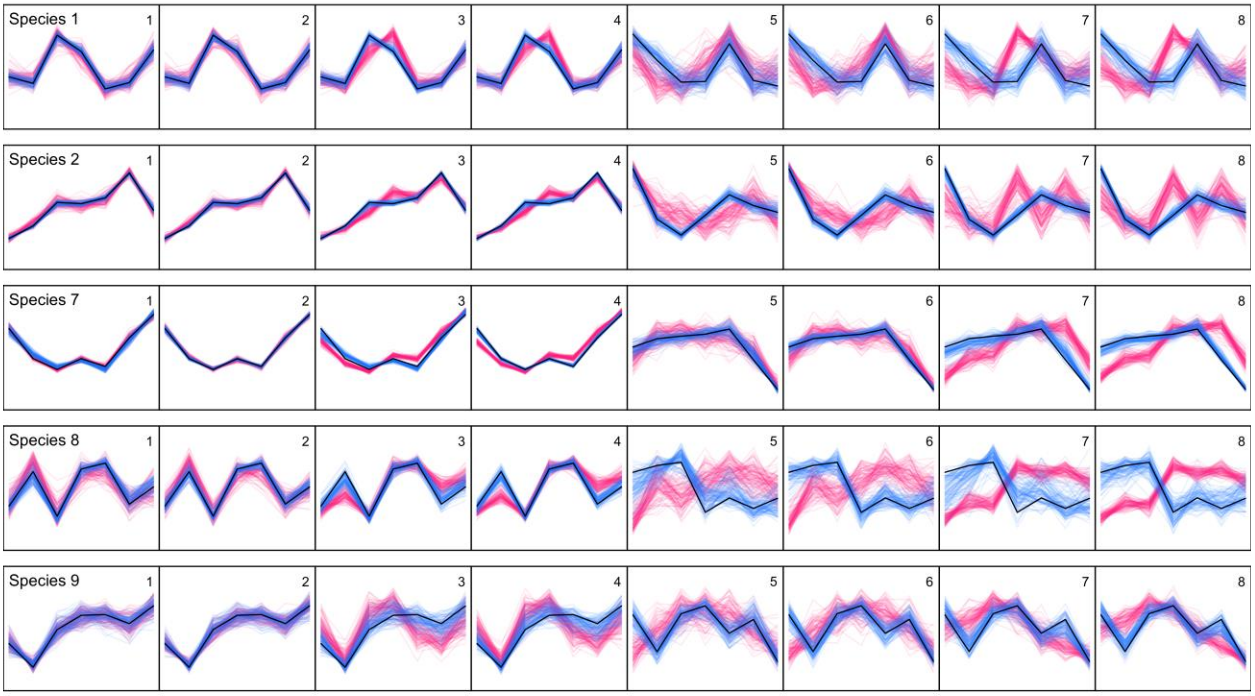
Species 1
1
2
3
4
5
6
7
8
Species 2
1
2
3
4
5
6
7
8
Species 7
1
2
3
4
5
6
7
8
Species 8
1
2
3
4
5
6
7
8
Species 9
1
2
3
4
5
6
7
8

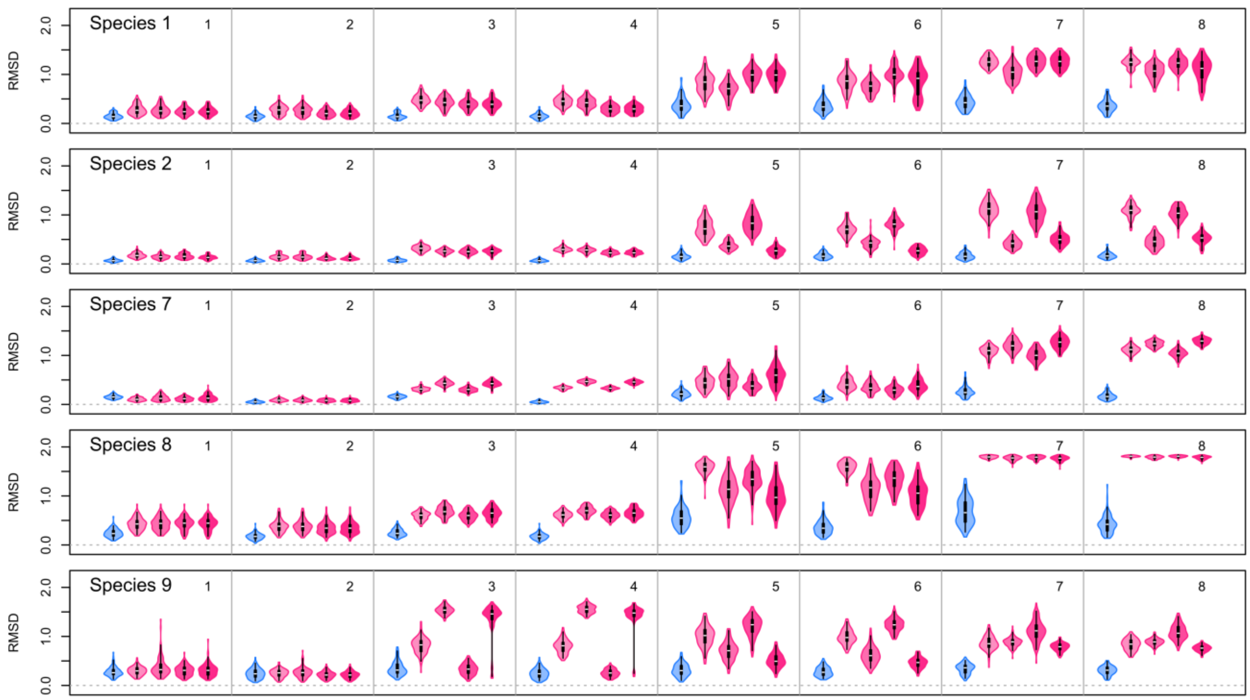

Species 1
Species 2
Species 7
Species 8
Species 9
1
2
3
4
5
6
7
8
RMSD
0.0
1.0
2.0

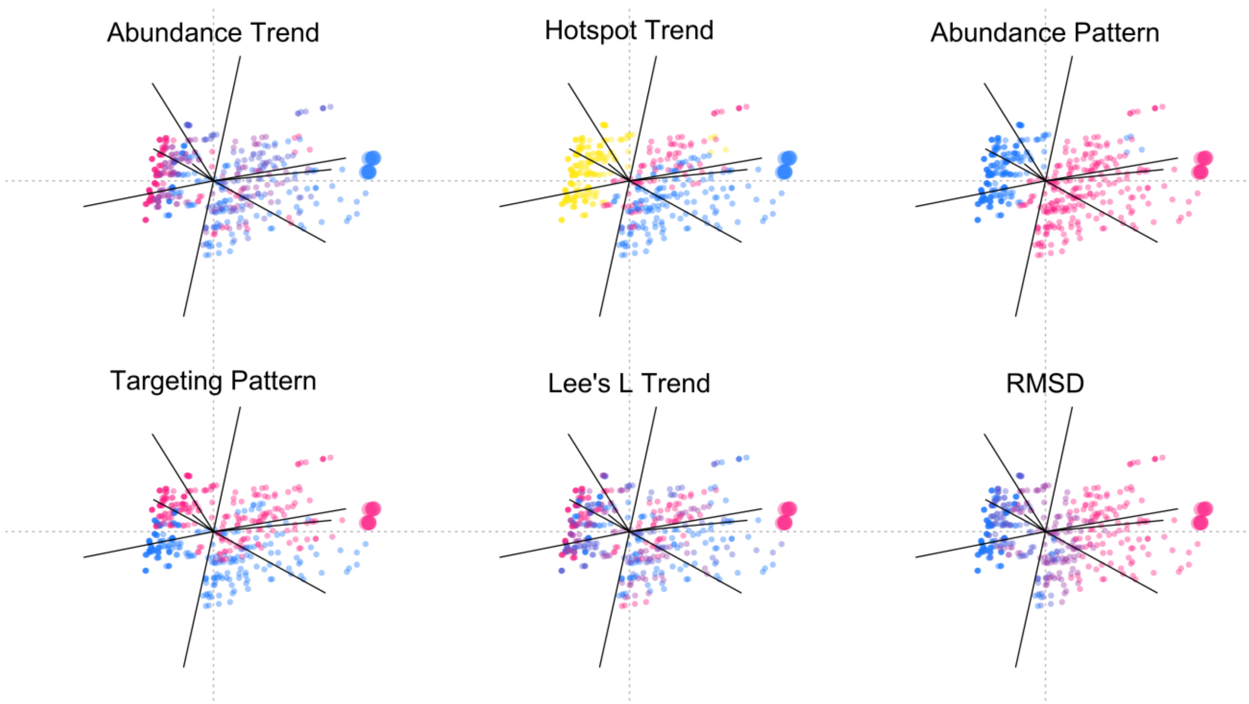
Abundance Trend
Hotspot Trend
Abundance Pattern
Targeting Pattern
Lee's L Trend
RMSD

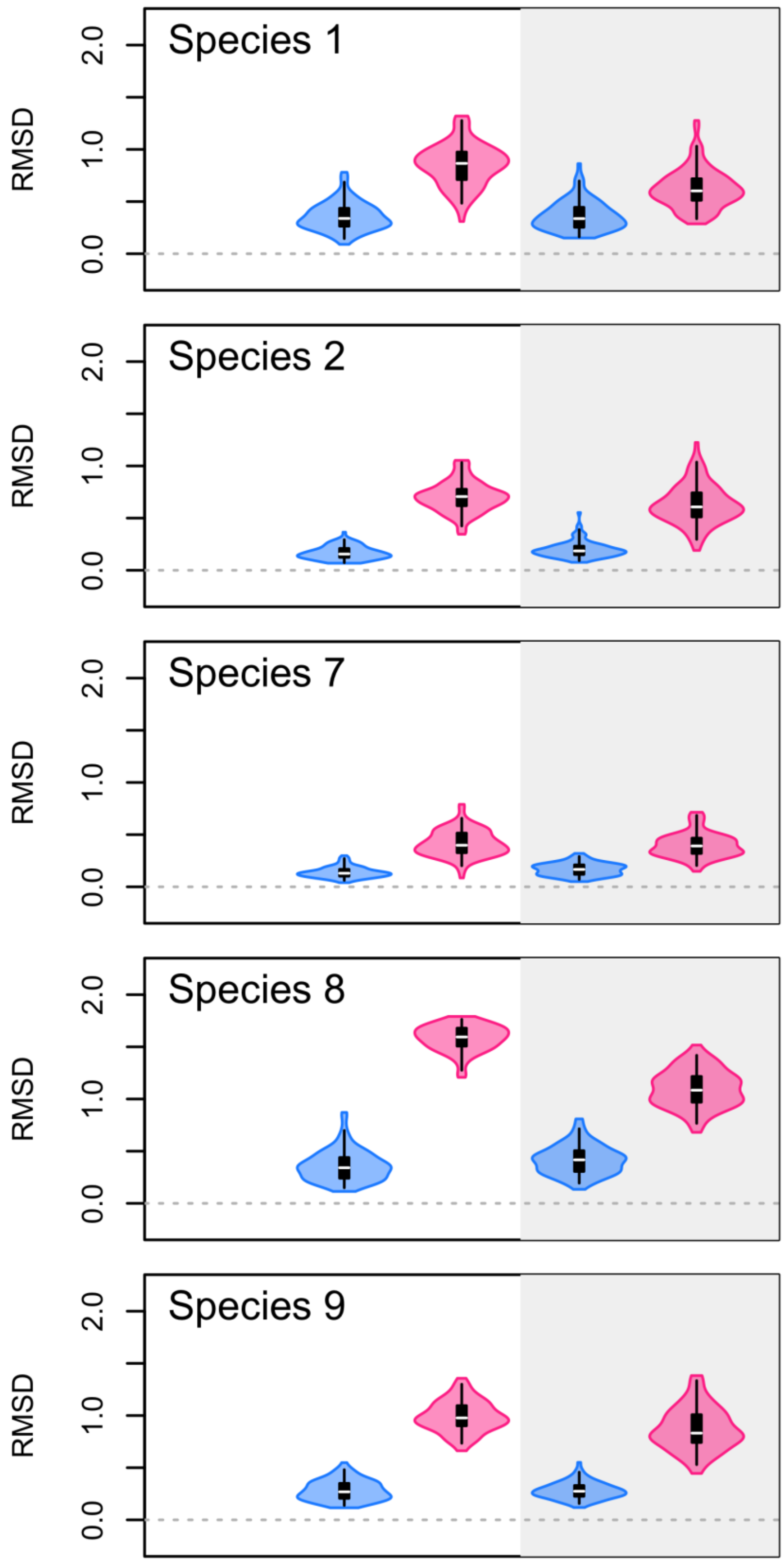
Species 1
Species 2
Species 7
Species 8
Species 9
RMSD
0.0
1.0
2.0

957

958

Table 1 Species occurring in the top 25 of catch by the vertical line fleet. The * indicates species in the Gulf of Mexico Reef Fish Management Plan, and the # indicates species removed from the analysis.

Scientific Name	Common Name
Balistes capriscus	Gray Triggerfish *
Calamus leucosteus	Whitebone Porgy
Calamus nodosus	Knobbed Porgy
Caranx crysos	Blue Runner
Caranx ruber	Bar Jack
Epinephelus flavolimbatus	Yellowedge Grouper *
Epinephelus morio	Red Grouper *
Epinephelus nigritus	Warsaw Grouper *
Epinephelus niveatus	Snowy Grouper *
Lachnolaimus maximus	Hogfish *
Lutjanus analis	Mutton Snapper *
Lutjanus campechanus	Red Snapper *
Lutjanus griseus	Mangrove Snapper *
Lutjanus synagris	Lane Snapper *
Lutjanus vivanus	Silk Snapper *
Mycteroperca bonaci	Black Grouper *
Mycteroperca microlepis	Gag Grouper *
Mycteroperca phenax	Scamp *
Ocyurus chrysurus	Yellowtail Snapper*
Pagrus pagrus	Red Porgy
Rachycentron canadum	Cobia #
Rhomboplites aurorubens	Vermilion Snapper *
Scomberomorus cavalla	King Mackerel #
Seriola dumerili	Greater Amberjack *
Seriola rivoliana	Almaco Jack *

Table 2 The 15 species used to inform the simulation and their approximate geographic distribution denoted as proportion of abundance in each region.

Number	Species	WGOM	NGOM	NEGOM	SEGOM
1	Red Grouper	0.00	0.03	0.52	0.45
2	Gag Grouper	0.07	0.12	0.60	0.21
3	Black Grouper	0.20	0.07	0.31	0.43
4	Warsaw Grouper	0.85	0.06	0.05	0.04
5	Snowy Grouper	0.26	0.21	0.18	0.35
6	Yellowedge Grouper	0.58	0.10	0.11	0.21
7	Red Snapper	0.83	0.14	0.02	0.01
8	Vermilion Snapper	0.65	0.29	0.05	0.01
9	Yellowtail Snapper	0.02	0.00	0.00	0.98
10	Mangrove Snapper	0.35	0.12	0.26	0.27
11	Mutton Snapper	0.00	0.01	0.00	0.97
12	Red Porgy	0.15	0.48	0.28	0.09
13	Gray Triggerfish	0.54	0.27	0.10	0.09
14	Whitebone Porgy	0.06	0.75	0.17	0.03
15	Hogfish	0.00	0.03	0.82	0.15

Table 3 Description of each scenario used in the simulation.

Scenario	Abundance Pattern	Effort Distribution	Targeting Shift
1	Global	Restricted	No
2	Global	Unrestricted	No
3	Global	Restricted	Yes
4	Global	Unrestricted	Yes
5	Local	Restricted	No
6	Local	Unrestricted	No
7	Local	Restricted	Yes
8	Local	Unrestricted	Yes

Table 4 Description of variables used in PCA

Variable	Description
1 - Species abundance trend	The slope of the true trend in abundance.
2 - Species hotspot trend	The slope of the trend in the annual number of cells that had abundance values greater than or equal to 2/3 of the maximum abundance value.
3 - Correlation with true trend	The time series correlation between the estimated trend and the true trend as described in section 2.4.
4 - Pseudo-significance of correlation to the true trend	The pseudo-significance of correlation to the true trend as described in section 2.4.
5 - Average annual Lee's L correlation between the distributions of effort and species abundance	Lee's L is a bivariate measure of the spatial correlation between two distributions (Lee 2001). Lee's L is bounded between -1 and 1 with values greater than 0 indicating a positive correlation.
6 - Trend in Lee's L correlation between the distributions of effort and species abundance	The slope of the trend in the annual Lee's L correlation between the distributions of effort and species abundance.
7 - Abundance pattern	A binary variable indicating either a global or local abundance pattern.
8 - Targeting shift	A binary variable indicating the presence or absence of a spatial targeting shift.
9 – Root-mean-square deviation	The RMSD between the estimated and true trend calculated as shown in Eq. 13.

Table 5 The metrics of agreement, mean correlation and mean inferred change in stock abundance, and their respective overlapping coefficients (OVLs) between the two estimated indices of abundance for each species arranged in order (highest to lowest) of proportion of fleet-wide catch.

Common Name	Correlation	OVL_{Corr}	$Change_{VMS}$	$Change_{GLM}$	OVL_{Change}
Red Snapper	0.85	0.05	2.23	1.53	0.04
Vermilion Snapper	0.41	0.34	-1.64	-0.30	0.00
Red Grouper	0.51	0.27	2.19	0.31	0.00
Gag Grouper	0.97	0.01	-1.75	-1.86	0.72
Yellowtail Snapper	0.44	0.73	-1.09	0.04	0.53
Greater Amberjack	-0.03	0.92	-0.13	-1.30	0.43
Red Porgy	-0.55	0.33	1.80	-2.08	0.00
Scamp	0.69	0.17	-1.02	-1.72	0.17
Mangrove Snapper	-0.57	0.28	1.67	-1.00	0.00
Black Grouper	0.95	0.09	-1.85	-1.87	0.60
Lane Snapper	0.33	0.67	0.45	-0.60	0.38
Whitebone Porgy	-0.14	0.69	-2.04	0.06	0.06
Gray Triggerfish	0.86	0.09	-2.22	-1.96	0.63
Warsaw Grouper	0.67	0.32	2.05	2.02	0.78
Snowy Grouper	-0.25	0.75	1.80	-1.55	0.05
Yellowedge Grouper	-0.28	0.70	1.84	-1.93	0.03
Almaco Jack	0.45	0.50	1.90	0.50	0.10
Silk Snapper	-0.32	0.76	-0.17	0.47	0.70
Bar Jack	0.55	0.59	2.23	1.62	0.23
Hogfish	0.58	0.51	1.78	1.18	0.40
Knobbed Porgy	-0.42	0.81	-1.38	1.50	0.20
Blue Runner	0.24	0.81	2.25	0.77	0.62
Mutton Snapper	0.57	0.68	2.30	1.11	0.40